

Polarisation effects in the central exclusive χ_c production and the J/ψ angular distributions*

Roman Pasechnik[†]

*Department of Physics and Astronomy,
Uppsala University, Box 516, SE-751 20 Uppsala, Sweden*

Antoni Szczurek[‡]

*Institute of Nuclear Physics PAN, PL-31-342 Cracow, Poland and
University of Rzeszów, PL-35-959 Rzeszów, Poland*

Oleg Teryaev[§]

Bogoliubov Laboratory of Theoretical Physics, JINR, Dubna 141980, Russia

(Dated: November 8, 2018)

Abstract

We discuss exclusive elastic double diffractive axial-vector $\chi_c(1^+)$ and tensor $\chi_c(2^+)$ mesons production for different meson polarisations in proton-(anti)proton collisions at the Tevatron energy. The amplitude for the process is derived within the k_t -factorisation approach using unintegrated gluon distributions (UGDFs). Differential cross sections for different χ_c polarisations are calculated. Angular distributions of J/ψ meson from the radiative $\chi_c(1^+, 2^+)$ decays are derived. Prospects for experimental selection of different spin states of χ_c mesons are discussed.

PACS numbers: 13.87.Ce, 13.60.Le, 13.85.Lg

* Dedicated to the memory of Alexei Kaidalov who passed away on July 25th, 2010

[†]Electronic address: roman.pasechnik@fysast.uu.se

[‡]Electronic address: antoni.szczurek@ifj.edu.pl

[§]Electronic address: teryaev@theor.jinr.ru

I. INTRODUCTION

Recently, the central exclusive production of χ_c charmonia has attracted a lot of attention from both experimental [1–3] and theoretical [4, 5] sides. At the moment, such a process provides the unique opportunity to test the QCD diffractive Kaidalov-Khoze-Martin-Ryskin (KKMR) mechanism [6] based on the k_t -factorisation incorporating nonperturbative small- x gluon dynamics described by the unintegrated gluon distribution functions (UGDFs) against accessible data.

The final hadronic central system is, however, rather complicated and composed of three spin states $\chi_c(0^+, 1^+, 2^+)$, and there is no yet any reliable way to measure them separately. Such a measurement would significantly reduce an overall theoretical uncertainty, as different χ_c spin contributions come from different phase space regions [7–9]. Indeed, in the asymptotical forward limit $\chi_c(1^+, 2^+)$ are strongly suppressed with respect to $\chi_c(0^+)$ due to the $J_z = 0$ selections rule [11]. However, corrections to this asymptotics turn out to be important in the total cross section leading to a noticeable contribution of the $\chi_c(1^+, 2^+)$ states to the observable signal from radiative χ_c decays [4, 7, 8]. Generally, separate measurements of χ_c states in diffractive production would impose more strict bounds on the production mechanism under consideration and extract some new information on the underlying QCD dynamics [5, 8].

One of the ways is to measure the characteristic differential distributions like meson p_\perp distributions or angular correlations of the outgoing protons. However, such distributions are rather sensitive to UGDFs and cuts on kinematical variables [7, 8], and existing experimental techniques do not allow to reconstruct such observables with sufficient precision. Another possible way is to look at observables related with meson polarisations and their decay distributions.

The goal of the present paper is to analyze polarisation effects in the central exclusive production of χ_c charmonia. Such effects can be potentially identified by measuring the angular distribution of J/ψ mesons from radiative decays of $\chi_c(J^+)$ giving more detailed information on the partial meson helicity contributions. Moreover, certain combinations of polarisation observables can be less sensitive to unknown nonperturbative effects leading to unique opportunities for model-independent analysis of diffractive processes.

The paper is organized as follows. In Section II we give general expressions for the amplitude of the central exclusive $\chi_c(1^+, 2^+)$ production with all necessary notations. Section III contains discussion of the rapidity dependence of the hard subprocess amplitudes for different χ_c polarisations. In Sections IV and V we derive the angular dependence of outgoing J/ψ mesons in the helicity frame in terms of the diffractive χ_c production density matrix $\rho_{\lambda\lambda'}$. Sections VI and VII are devoted to discussion of gluon off-shell effects and absorptive corrections. Section VIII contains the presentation of the main results, including differential distributions of polarised $\chi_c(1^+, 2^+)$ and angular correlations of the outgoing J/ψ mesons. Finally, in Section IX we give a set of concluding remarks and present a discussion of the final results and theoretical uncertainties.

II. AMPLITUDES OF EXCLUSIVE P-WAVE CHARMONIA PRODUCTION

According to the Kaidalov-Khoze-Martin-Ryskin approach (KKMR) [6], we write the amplitude of the exclusive double diffractive color singlet production $pp \rightarrow pp\chi_{cJ}$ as

$$\mathcal{M}_{J,\lambda}^{g^*g^*} = \frac{s}{2} \cdot \pi^2 \frac{\delta_{c_1 c_2}}{N_c^2 - 1} \Im \int d^2 q_{0,t} V_{J,\lambda}^{c_1 c_2} \frac{f_{g,1}^{\text{off}}(x_1, x'_1, q_{0,t}^2, q_{1,t}^2, t_1) f_{g,2}^{\text{off}}(x_2, x'_2, q_{0,t}^2, q_{2,t}^2, t_2)}{q_{0,t}^2 q_{1,t}^2 q_{2,t}^2}, \quad (2.1)$$

where $f_{g,i}^{\text{off}}(x_i, x'_i, q_{0,t}^2, q_{i,t}^2, t_i)$ are the off-diagonal unintegrated gluon distributions for “active” gluons with momenta $q_i = x_i p_i + q_{i,t}$ and color indices c_i , and the screening soft gluon with small fraction $x' \ll x_i$, $q_0 \simeq q_{0,t}$, J and λ are the spin and helicity of a produced meson with momentum $P = q_1 + q_2$ and mass M in the center-of-mass frame of colliding protons and z axis directed along the meson momentum \mathbf{P} , respectively. $V_{J,\lambda}^{c_1 c_2}$ here is the hard $g^*g^* \rightarrow \chi_{cJ}$ production amplitude for charmonium with quantum numbers J, λ .

The structure of V_J in Eq. (2.1) (we omit here the color and polarisation indices for simplicity) is determined by gauge invariant amplitude $V_J^{\mu\nu}$ for the off-shell gluon fusion process, and given in terms of its projection onto the gluon polarisation vectors as [7–9]

$$V_J = n_\mu^+ n_\nu^- V_J^{\mu\nu} = \frac{4}{s} \frac{q_{1,t}^\nu}{x_1} \frac{q_{2,t}^\mu}{x_2} V_{J,\mu\nu}, \quad q_1^\nu V_J^{\mu\nu} = q_2^\mu V_{J,\mu\nu} = 0. \quad (2.2)$$

In order to define the polarisation states of $\chi_c(1^+, 2^+)$ mesons, one has to fix a specific frame, in which those are uniquely identified and can be measured experimentally. The commonly used polarisation frames are the helicity, target, Gottfried-Jackson and Collins-Soper frames (see, e.g. [10]). In this work we primarily focus on polarisation effects in the helicity frame.

According to Refs. [7, 8], in the considered frame we introduce the time-like basis vectors $n_{1,2,3}$ satisfying $n_\alpha^\mu n_\beta^\nu g_{\mu\nu} = g_{\alpha\beta}$ (with $n_0^\mu = P_\mu/M$) with collinear \mathbf{n}_3 and \mathbf{P} vectors (so, we have $\mathbf{P} = (E, 0, 0, P_z)$, $P_z = |\mathbf{P}| > 0$), and

$$n_1^\beta = (0, 1, 0, 0), \quad n_2^\beta = (0, 0, 1, 0), \quad n_3^\beta = \frac{1}{M} (|\mathbf{P}|, 0, 0, E), \quad |\mathbf{P}| = \sqrt{E^2 - M^2}. \quad (2.3)$$

Then the hard production amplitudes for the axial-vector $J = 1$ ($\lambda = 0, \pm 1$) and tensor $J = 2$ ($\lambda = 0, \pm 1, \pm 2$) charmonia in the helicity frame read (for more details, see Refs. [7, 8])

$$\begin{aligned} V_{J=1,\lambda}^{c_1 c_2} = & -8g^2 \delta^{c_1 c_2} \sqrt{\frac{6}{M\pi N_c}} \frac{\mathcal{R}'(0)}{|\mathbf{P}_t|(M^2 - q_{1,t}^2 - q_{2,t}^2)^2} \left\{ \frac{1}{\sqrt{2}} \left[i|\lambda|(q_{1,t}^2 - q_{2,t}^2)(q_{1,t} q_{2,t}) \text{sign}(\sin \psi) + \right. \right. \\ & \left. \lambda(q_{1,t}^2 + q_{2,t}^2) |[\mathbf{q}_{1,t} \times \mathbf{q}_{2,t}] \times \mathbf{n}_1| \text{sign}(Q^y) \text{sign}(\cos \psi) \right] + \\ & \left. (1 - |\lambda|)(q_{1,t}^2 + q_{2,t}^2) |[\mathbf{q}_{1,t} \times \mathbf{q}_{2,t}] \times \mathbf{n}_3| \text{sign}(Q^y) \text{sign}(\sin \psi) \right\}, \end{aligned} \quad (2.4)$$

$$\begin{aligned}
V_{J=2,\lambda}^{c_1 c_2} = & 2ig^2 \delta^{c_1 c_2} \sqrt{\frac{1}{3M\pi N_c}} \frac{\mathcal{R}'(0)}{M|\mathbf{P}_t|^2(M^2 - q_{1,t}^2 - q_{2,t}^2)^2} \times \\
& \left[6M^2 i|\lambda|(q_{1,t}^2 - q_{2,t}^2) \text{sign}(Q^y) \left\{ |[\mathbf{q}_{1,t} \times \mathbf{q}_{2,t}] \times \mathbf{n}_1| (1 - |\lambda|) \text{sign}(\sin \psi) \text{sign}(\cos \psi) + \right. \right. \\
& 2|[\mathbf{q}_{1,t} \times \mathbf{q}_{2,t}] \times \mathbf{n}_3| (2 - |\lambda|) \left. \right\} - [2q_{1,t}^2 q_{2,t}^2 + (q_{1,t}^2 + q_{2,t}^2)(q_{1,t} q_{2,t})] \times \\
& \left\{ 3M^2 (\cos^2 \psi + 1) \lambda (1 - |\lambda|) + 6ME \sin(2\psi) \lambda (2 - |\lambda|) \text{sign}(\sin \psi) \text{sign}(\cos \psi) + \right. \\
& \left. \left. \sqrt{6} (M^2 + 2E^2) \sin^2 \psi (1 - |\lambda|)(2 - |\lambda|) \right\} \right], \tag{2.5}
\end{aligned}$$

where $\pm Q^y$ are the y -components of the gluon transverse momenta $q_{1/2,t}$ in considered coordinates, $\psi = [0 \dots \pi]$ is the polar angle between \mathbf{P} and the c.m.s. beam axis, and

$$\begin{aligned}
|[\mathbf{q}_{1,t} \times \mathbf{q}_{2,t}] \times \mathbf{n}_1| &= \sqrt{q_{1,t}^2 q_{2,t}^2 - (q_{1,t} q_{2,t})^2} |\cos \psi|, \\
|[\mathbf{q}_{1,t} \times \mathbf{q}_{2,t}] \times \mathbf{n}_3| &= \frac{E}{M} \sqrt{q_{1,t}^2 q_{2,t}^2 - (q_{1,t} q_{2,t})^2} |\sin \psi|, \\
|\mathbf{P}_t|^2 &= |\mathbf{q}_{1,t}|^2 + |\mathbf{q}_{2,t}|^2 + 2|\mathbf{q}_{1,t}||\mathbf{q}_{2,t}| \cos \phi,
\end{aligned}$$

where ϕ is the angle between fusing gluons. Amplitudes (2.4) and (2.5) explicitly obey gauge invariance and Bose symmetry properties with respect to the gluon momenta interchange $q_1 \leftrightarrow q_2$.

Another important feature is that the amplitude of axial-vector charmonia production turns to zero for on-shell gluons, i.e. when $q_{1,t}^2 = 0$, $q_{2,t}^2 = 0$ due to the Landau-Yang theorem (see, e.g. Ref. [7]). The gluon virtualities (transverse momenta) provide a leading effect in the diffractive $\chi_c(1^+)$ production, and, therefore, cannot be neglected [4, 7]. This is the striking difference between the k_t -factorisation approach under consideration and collinear factorisation which forbids production of axial-vector states [7].

As was demonstrated in Refs. [7, 8] amplitudes for diffractive $\chi_c(1^+, 2^+)$ turn to zero in the forward limit, i.e. when $\mathbf{q}_{1,t} = -\mathbf{q}_{2,t} = \mathbf{q}_{0,t}$, due to symmetry relations. This is a direct consequence of $J_z = 0$ selection rule [11] saying that CEP of higher spins $J = 1, 2, \dots$ is strongly suppressed in the forward limit. Like the gluon virtualities in the $\chi_c(1^+)$ case, the off-forward corrections provide a leading effect in the case of $\chi_c(1^+, 2^+)$ production, and cannot be neglected in the integrated cross section. In particular, they lead to a substantial contribution of $\chi_c(2^+)$ meson CEP [8], close to that from $\chi_c(0^+, 1^+)$ mesons.

Let us now turn to the discussion of the polarisation effects in diffractive $1^+, 2^+$ charmonia production and first start from analytic investigation of helicity amplitudes.

III. RAPIDITY DEPENDENCE OF $g^* g^* \rightarrow \chi_c(J)$ AMPLITUDES SQUARED

For the purpose of illustration¹, it is interesting to look at the y -dependence of the $g^* g^* \rightarrow \chi_c(J = 1, 2)$ (hard) subprocess amplitudes (2.4) and (2.5) for different meson helic-

¹ Please, note that the content of this Section aims to analytical illustration of specific rapidity dependence of the hard subprocess $g^* g^* \rightarrow \chi_c$ amplitudes squared, not the diffractive $pp \rightarrow pp \chi_c$ amplitude squared.

ities $\lambda = 0, \pm 1$ and $\lambda = 0, \pm 1, \pm 2$, respectively. It is convenient to express them in terms of the transverse 3-momenta of fusing off-shell gluons $|\mathbf{q}_{1,t}|$ and $|\mathbf{q}_{2,t}|$, and the angle between them ϕ in the center-of-mass frame of colliding nucleons with the z -axis fixed along meson momentum \mathbf{P} . In this case, summing the matrix element squared $|V_\lambda^J|^2$ over meson polarisations λ up to some constant normalization factor N^J we get:

$$\begin{aligned} S^{J=1} &= N^{J=1} \frac{|\mathbf{q}_{1,t}|^2 |\mathbf{q}_{2,t}|^2 \left[(|\mathbf{q}_{1,t}|^2 + |\mathbf{q}_{2,t}|^2)^2 \sin^2 \phi + M^2 (|\mathbf{q}_{1,t}|^2 + |\mathbf{q}_{2,t}|^2 - 2|\mathbf{q}_{1,t}||\mathbf{q}_{2,t}| \cos \phi) \right]}{(|\mathbf{q}_{1,t}|^2 + |\mathbf{q}_{2,t}|^2 + M^2)^4}, \\ S^{J=2} &= N^{J=2} \frac{|\mathbf{q}_{1,t}|^2 |\mathbf{q}_{2,t}|^2 \left[3M_\perp^2 M^2 + (|\mathbf{q}_{1,t}|^2 \cos \phi + |\mathbf{q}_{2,t}|^2 \cos \phi + 2|\mathbf{q}_{1,t}||\mathbf{q}_{2,t}|)^2 \right]}{(|\mathbf{q}_{1,t}|^2 + |\mathbf{q}_{2,t}|^2 + M^2)^4} \end{aligned} \quad (3.1)$$

These sums are proportional to the ones derived by Kniehl et al. in Ref. [12] (see right below Eq. (27)). The distinction is only due to different normalizations of gluon polarisation vectors $\epsilon_\mu = q_{1/2,t}^\mu / |\mathbf{q}_{1/2,t}|$ used in Ref. [12] and light-cone vectors n_μ^\pm used in our calculation. The sums (3.1) are y -independent. Then, for partial polarisations of the $\chi_c(1^+)$ meson we have

$$\begin{aligned} |V_{\lambda=0}^{J=1}|^2 &= S^{J=1} \frac{\mathcal{A} M_\perp^2 \cosh^2 y}{(M_\perp^2 \cosh^2 y - M^2)(\mathcal{B} M^2 + \mathcal{A})}, \\ |V_{\lambda=\pm 1}^{J=1}|^2 &= \frac{S^{J=1}}{2} \frac{M^2 [\mathcal{B}(M_\perp^2 \cosh^2 y - M^2) - \mathcal{A}]}{(M_\perp^2 \cosh^2 y - M^2)(\mathcal{B} M^2 + \mathcal{A})}, \end{aligned} \quad (3.2)$$

where

$$\mathcal{A} = (|\mathbf{q}_{1,t}|^2 + |\mathbf{q}_{2,t}|^2)^2 \sin^2 \phi, \quad \mathcal{B} = |\mathbf{q}_{1,t}|^2 + |\mathbf{q}_{2,t}|^2 - 2|\mathbf{q}_{1,t}||\mathbf{q}_{2,t}| \cos \phi.$$

Analogously, for the tensor $\chi_c(2^+)$ meson we have

$$\begin{aligned} |V_{\lambda=0}^{J=2}|^2 &= S^{J=2} \frac{\mathcal{R} [M_\perp^4 \cosh 4y + 4(M_\perp^2 + M^2) M_\perp^2 \cosh 2y + 3M_\perp^4 + 4M_\perp^2 M^2 + 2M^4]}{\mathcal{Q}(M_\perp^4 \cosh 4y + 4\mathcal{M} \cosh 2y + 3M_\perp^4 - 8M^2 |\mathbf{P}_\perp|^2)}, \\ |V_{\lambda=\pm 1}^{J=2}|^2 &= \frac{S^{J=2}}{2} \frac{3M_\perp^2 M^2 [|\mathbf{P}_\perp|^2 M_\perp^2 \cosh 4y + 4\mathcal{P}(\cosh 2y + 1) - |\mathbf{P}_\perp|^2 M_\perp^2]}{\mathcal{Q}(M_\perp^4 \cosh 4y + 4\mathcal{M} \cosh 2y + 3M_\perp^4 - 8M^2 |\mathbf{P}_\perp|^2)}, \\ |V_{\lambda=\pm 2}^{J=2}|^2 &= \frac{S^{J=2}}{2} \frac{3M^4 [M_\perp^4 (\cosh 4y + 1) - 4M^2 M_\perp^2 \cosh 2y - 2\mathcal{P} + 2M^4]}{\mathcal{Q}(M_\perp^4 \cosh 4y + 4\mathcal{M} \cosh 2y + 3M_\perp^4 - 8M^2 |\mathbf{P}_\perp|^2)}, \end{aligned} \quad (3.3)$$

where for compactness we have introduced the following short-hand notations:

$$\begin{aligned} \mathcal{R} &= (|\mathbf{q}_{1,t}|^2 \cos \phi + |\mathbf{q}_{2,t}|^2 \cos \phi + 2|\mathbf{q}_{1,t}||\mathbf{q}_{2,t}|)^2, \\ \mathcal{Q} &= 3M_\perp^2 M^2 + \mathcal{R}, \quad \mathcal{P} = |\mathbf{P}_\perp|^4 - \mathcal{R}, \quad \mathcal{M} = |\mathbf{P}_\perp|^4 - M^4. \end{aligned}$$

For illustration in Fig. 1 we show the helicity amplitudes squared as a function of meson rapidity at some fixed kinematical point. Apparently, they obey a quite non-trivial strong y -dependence in the vicinity of $y = 0$ which will result in the “peaked” structure (maxima/minima) of the differential cross sections $d\sigma_\lambda^J/dy$ of double diffractive polarised $\chi_c(1^+, 2^+)$ production (see Results section).

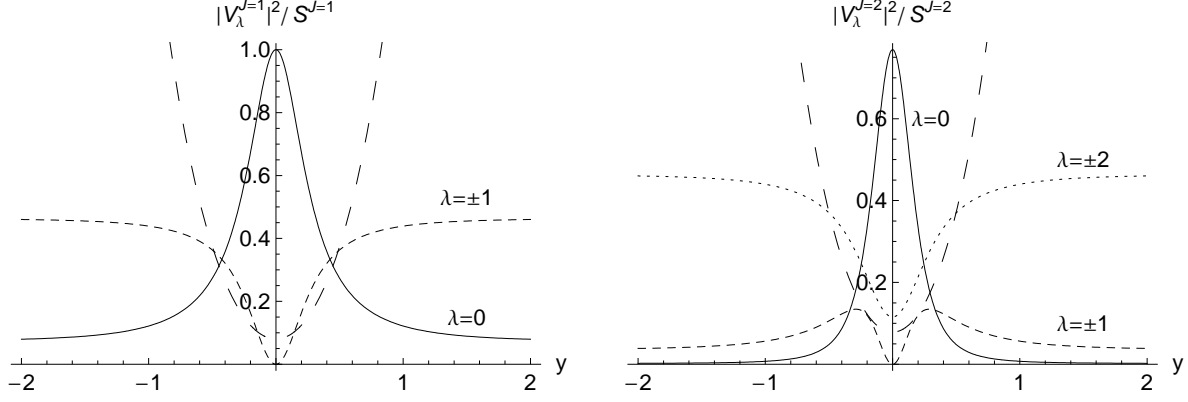


FIG. 1: Illustration of the meson rapidity dependence of the normalized subprocess $g^*g^* \rightarrow \chi_c(1^+)$ (left panel) and $g^*g^* \rightarrow \chi_c(2^+)$ (right panel) amplitudes squared for different meson helicities λ at arbitrarily fixed kinematical variables $|\mathbf{q}_{1,t}| = |\mathbf{q}_{1,t}| = 0.5$ GeV and $\phi = 0.2$.

It follows from Eqs. (3.2) and (3.3) that in the forward limit, corresponding to $\mathbf{q}_{1,t} = -\mathbf{q}_{2,t}$, helicity amplitudes $V_{\lambda=0}^{J=1}$ and $V_{\lambda=0,\pm 1}^{J=2}$ turn to zero. So, the total signal is dominated only by maximal helicity contributions, i.e. by $\lambda = \pm 1$ for $\chi_c(1^+)$ and $\lambda = \pm 2$ for $\chi_c(2^+)$. Therefore, nontrivial “peaked” rapidity dependence of the cross section around $y = 0$, as long as absolute values of non-maximal λ contributions, can be served as a measure of non-forward corrections in the production process.

Let us consider how to measure such polarisation effects in radiative decay channel $\chi_c(1^+, 2^+) \rightarrow J/\psi + \gamma$ and understand how these effects manifest themselves in differential distributions of outgoing J/ψ meson.

IV. DIFFRACTIVE χ_{cJ} PRODUCTION DENSITY MATRIX

The cross section for the unpolarised χ_{cJ} production in the 3-body reaction $pp \rightarrow pp\chi_{cJ}$, where $J = 1, 2$, can be written as

$$\sigma_{\chi_c}^J = \sum_{\lambda=-J}^J \sigma_{\lambda\lambda}^J, \quad \sigma_{\lambda\lambda'}^J = \sigma_{\chi_c}^J \cdot \rho_{\lambda\lambda}^J = \frac{1}{2s} \int d^3PS \cdot d\sigma_{\lambda\lambda'}(\{\dots\}), \quad (4.1)$$

where $\rho_{\lambda\lambda'}^J$ is the hermitian helicity density matrix $\rho_{\lambda\lambda'}^{J*} = \rho_{\lambda'\lambda}^J$. In the differential form it can be written in terms of invariant diffractive amplitude as

$$d\rho_{\lambda\lambda'}(\{\dots\}) \equiv \frac{d\sigma_{\lambda\lambda'}}{\sigma_{\chi_c}^J} = \frac{1}{\sigma_{\chi_c}^J} \cdot \frac{1}{4} \sum_{\bar{\lambda}_1, \bar{\lambda}_2, \bar{\lambda}'_1, \bar{\lambda}'_2} \mathcal{M}_{\bar{\lambda}_1 \bar{\lambda}_2 \rightarrow \bar{\lambda}'_1 \bar{\lambda}'_2 \lambda}^*(\{\dots\}) \mathcal{M}_{\bar{\lambda}_1 \bar{\lambda}_2 \rightarrow \bar{\lambda}'_1 \bar{\lambda}'_2 \lambda'}(\{\dots\}). \quad (4.2)$$

Above $\{\dots\}$ is an abbreviation for a four-dimensional phase space point. In our case, because of nucleon helicity conservation ($\bar{\lambda}_1 = \bar{\lambda}'_1$, $\bar{\lambda}_2 = \bar{\lambda}'_2$), the nucleon helicities can be suppressed. In general, $\rho_{\lambda\lambda'}^J$ is a function of kinematical variables $(x_F, t_1, t_2, \phi_{pp})$ (or any other equivalent set of variables).

Invariance of the amplitude \mathcal{M} under reflection in the production plane by the action of the operator $\exp(-i\pi J_y)\mathcal{P}$, where \mathcal{P} is the parity operator, leads to the relation

$$\rho_{-\lambda, -\lambda'}^J = (-1)^{\lambda - \lambda'} \rho_{\lambda\lambda'}^J. \quad (4.3)$$

Thus, for example, in the case of $J = 1$ there are only four independent components in $\rho_{\lambda\lambda'}^J$: ρ_{00}^1 , ρ_{11}^1 , ρ_{10}^1 , and ρ_{-11}^1 . The diagonal elements of the density matrix are real.

V. ANGULAR DISTRIBUTION OF J/ψ MESON FROM $\chi_c(J)$ DECAY

Let us consider the central exclusive production process $pp \rightarrow pp\chi_{cJ}$ followed by the radiative decay $\chi_{cJ} \rightarrow J/\psi + \gamma$. We shall limit ourselves here to the narrow-width approximation. Below we follow notations in Ref. [13]. Let θ and ϕ be the polar and azimuthal angles of the J/ψ meson in the $\chi_c(J^+)$ rest frame (this is so-called helicity frame). Then, the differential cross section of the J/ψ production in the sequential process $pp \rightarrow pp(\chi_{cJ} \rightarrow J/\psi + \gamma)$ can be written as

$$\frac{d\sigma_{J/\psi}^J}{d\Omega} = B_J(\chi_{cJ} \rightarrow J/\psi\gamma) \cdot W(\theta, \phi), \quad W(\theta, \phi) = \sum_{\lambda, \lambda'=-J}^J \rho_{\lambda\lambda'}^J A_{\lambda\lambda'}^J(\theta, \phi), \quad (5.1)$$

where $d\Omega = d\cos\theta d\phi$, B_J denotes the branching fraction of $\chi_{cJ} \rightarrow J/\psi\gamma$, $W(\theta, \phi)$ is the angular distribution of the J/ψ meson, $\rho_{\lambda\lambda'}^J$ is the integrated density matrix corresponding to χ_{cJ} production process (4.1), and $A_{\lambda\lambda'}^J$ refers to the χ_{cJ} decay process and allows to describe the decay angular distribution

$$A_{\lambda\lambda'}^J(\theta, \phi) = \frac{\sum_{\lambda_1, \lambda_2} \langle \lambda_1, \lambda_2, \theta, \phi | T | J, \lambda' \rangle^* \langle \lambda_1, \lambda_2, \theta, \phi | T | J, \lambda \rangle}{\int \sum_{\lambda, \lambda_1, \lambda_2} |T_{\lambda, \lambda_1, \lambda_2}^J(\theta, \phi)|^2 d\Omega}, \quad (5.2)$$

where $\lambda_1 = 0, \pm 1$ and $\lambda_2 = \pm 1$ are the helicities of the J/ψ and γ in the χ_{cJ} rest frame, respectively. The transition matrix element of the radiative decay process $\chi_{cJ}(\lambda) \rightarrow J/\psi(\lambda_1, \theta, \phi) + \gamma(\lambda_2, \pi - \theta, \phi + \pi)$ in the considered frame of reference is [14]

$$\begin{aligned} \langle \lambda_1, \lambda_2, \theta, \phi | T | J, \lambda \rangle &= \sqrt{\frac{2J+1}{4\pi}} T_{\lambda_1, \lambda_2}^J D_{\lambda, \lambda_1 - \lambda_2}^{J*}(-\phi, \theta, \phi), \\ T_{\lambda_1, \lambda_2}^J &= \sqrt{\frac{4\pi}{2J+1}} \langle \lambda_1, \lambda_2, 0, 0 | T | J, \lambda \rangle|_{\lambda=\lambda_1-\lambda_2}, \end{aligned} \quad (5.3)$$

Let η , η_1 , and η_2 (J , J_1 , and J_2) are the parities (total angular momenta) of the χ_{cJ} , J/ψ , and γ , respectively. Angular-momentum conservation imposes the selection rule $|\lambda_1 - \lambda_2| \leq J$. Due to the parity conservation the decay amplitude $T_{\lambda_1, \lambda_2}^J$ satisfies the following symmetry property [14]

$$T_{-\lambda_1, -\lambda_2}^J = \eta\eta_1\eta_2(-1)^{J_1+J_2-J} T_{\lambda_1, \lambda_2}^J = (-1)^J T_{\lambda_1, \lambda_2}^J. \quad (5.4)$$

Thus, an independent set of $T_{\lambda_1, \lambda_2}^J$ components for $J = 1, 2$ reads

$$J = 1: \quad t_0^1 \equiv T_{1,1}^1 = -T_{-1,-1}^1, \quad t_1^1 \equiv T_{0,-1}^1 = -T_{0,1}^1, \quad (5.5)$$

$$J = 2: \quad t_0^2 \equiv T_{1,1}^2 = T_{-1,-1}^2, \quad t_1^2 \equiv T_{0,-1}^2 = T_{0,1}^2, \quad t_2^2 \equiv T_{1,-1}^2 = T_{-1,1}^2. \quad (5.6)$$

The matrix

$$D_{m'm}^j(\alpha, \beta, \gamma) = \langle j, m' | D(\alpha, \beta, \gamma) | j, m \rangle = \exp(-i\gamma m') d_{m'm}^j(\beta) \exp(-i\alpha m) \quad (5.7)$$

is the representation of the rotation operator

$$D(\alpha, \beta, \gamma) = \exp(-i\gamma J_z) \exp(-i\beta J_y) \exp(-i\alpha J_x), \quad (5.8)$$

with α , β and γ being the Euler angles, in the eigenstates $|j, m\rangle$ of J^2 and J_z . The well-known d -functions $d_{m'm}^j(\beta) = \langle j, m' | \exp(-i\beta J_y) | j, m \rangle$ may be evaluated from the Wigner's formula [15]

$$\begin{aligned} d_{m'm}^j(\beta) &= \sum_{k=\max(0, m-m')}^{\min(j+m, j-m')} (-1)^{k-m+m'} \frac{\sqrt{(j+m)!(j-m)!(j+m')!(j-m')!}}{k!(k-m+m')!(j+m-k)!(j-m'-k)!} \times \\ &\times \left(\cos \frac{\beta}{2} \right)^{2j+m-m'-2k} \left(\sin \frac{\beta}{2} \right)^{2k-m+m'}. \end{aligned} \quad (5.9)$$

Orthogonality condition

$$\int d\Omega D_{m'm''}^j(-\phi, \theta, \phi) D_{mm''}^{j*}(-\phi, \theta, \phi) = \frac{4\pi}{2j+1} \delta_{m'm} \quad (5.10)$$

provides the normalization of $A_{\lambda, \lambda'}^J$

$$\int d\Omega A_{\lambda \lambda'}^J(\theta, \phi) = \delta_{\lambda \lambda'}, \quad (5.11)$$

so that, upon integration over the solid angle, Eq. (5.1) reduces to the narrow-width approximation formula

$$\sigma_{J/\psi}^J = B_J(\chi_{cJ} \rightarrow J/\psi + \gamma) \sigma_{\chi_c}^J. \quad (5.12)$$

Combining all above ingredients together, we get the angular distribution of the J/ψ meson (5.1) in the general form

$$\begin{aligned} W^{J=1}(\theta, \phi) &= \frac{3\sigma_{\chi_c}^{J=1}}{4\pi} \left\{ \rho_{0,0}^1 \left[r_0^1 \cos^2 \theta + \frac{r_1^1}{2} \sin^2 \theta \right] + \rho_{1,1}^1 \left[r_0^1 \sin^2 \theta + \frac{r_1^1}{2} (1 + \cos^2 \theta) \right] \right. \\ &\quad - \sqrt{2} \sin(2\theta) \left(r_0^1 - \frac{r_1^1}{2} \right) [\text{Re}(\rho_{1,0}^1) \cos \phi - \text{Im}(\rho_{1,0}^1) \sin \phi] \\ &\quad \left. - \sin^2 \theta \left(r_0^1 - \frac{r_1^1}{2} \right) [\text{Re}(\rho_{1,-1}^1) \cos(2\phi) - \text{Im}(\rho_{1,-1}^1) \sin(2\phi)] \right\}, \end{aligned} \quad (5.13)$$

$$\begin{aligned}
W^{J=2}(\theta, \phi) = & \frac{5\sigma_{\chi_c}^{J=2}}{4\pi} \left\{ \rho_{0,0}^2 \left[\frac{1}{4} r_0^2 (3 \cos^2 \theta - 1)^2 + \frac{3}{2} r_1^2 \sin^2 \theta \cos^2 \theta + \frac{3}{8} r_2^2 \sin^4 \theta \right] \right. \\
& + \rho_{1,1}^2 \left[3 r_0^2 \sin^2 \theta \cos^2 \theta + \frac{r_1^2}{2} (4 \cos^4 \theta - 3 \cos^2 \theta + 1) + \frac{r_2^2}{2} \sin^2 \theta (\cos^2 \theta + 1) \right] \\
& + \rho_{2,2}^2 \left[\frac{3}{4} r_0^2 \sin^4 \theta + \frac{r_1^2}{2} \sin^2 \theta (\cos^2 \theta + 1) + \frac{r_2^2}{8} (\cos^4 \theta + 6 \cos^2 \theta + 1) \right] \\
& + \frac{\sqrt{6}}{4} \sin 2\theta (2 r_0^2 (1 - 3 \cos^2 \theta) + 2 r_1^2 \cos 2\theta + r_2^2 \sin^2 \theta) [\text{Re}(\rho_{1,0}^2) \cos \phi - \text{Im}(\rho_{1,0}^2) \sin \phi] \\
& - \frac{1}{2} \sin^2 \theta (6 r_0^2 \cos^2 \theta + r_1^2 (\sin^2 \theta - 3 \cos^2 \theta) - r_2^2 \sin^2 \theta) [\text{Re}(\rho_{1,-1}^2) \cos 2\phi - \text{Im}(\rho_{1,-1}^2) \sin 2\phi] \\
& + \frac{1}{2} \sin^3 \theta (6 r_0^2 - 4 r_1^2 + r_2^2) \left[\cos \theta [\text{Re}(\rho_{2,-1}^2) \cos 3\phi - \text{Im}(\rho_{2,-1}^2) \sin 3\phi] \right. \\
& \quad \left. + \frac{1}{4} \sin \theta [\text{Re}(\rho_{2,-2}^2) \cos 4\phi - \text{Im}(\rho_{2,-2}^2) \sin 4\phi] \right] \\
& + \frac{\sqrt{6}}{4} \sin^2 \theta (2 r_0^2 (3 \cos^2 \theta - 1) - 4 r_1^2 \cos^2 \theta + r_2^2 (\cos^2 \theta + 1)) [\text{Re}(\rho_{2,0}^2) \cos 2\phi - \text{Im}(\rho_{2,0}^2) \sin 2\phi] \\
& \left. - \frac{1}{4} \sin 2\theta (6 r_0^2 \sin^2 \theta + 4 r_1^2 \cos^2 \theta - r_2^2 (\cos^2 \theta + 3)) [\text{Re}(\rho_{2,1}^2) \cos \phi - \text{Im}(\rho_{2,1}^2) \sin \phi] \right\}, \tag{5.14}
\end{aligned}$$

where

$$r_\lambda^J = \frac{|t_\lambda^J|^2}{\sum_{\lambda'=0}^J |t_{\lambda'}^J|^2} \tag{5.15}$$

are positive numbers satisfying $\sum_{\lambda=0}^J r_\lambda^J = 1$ to be determined experimentally. In Ref. [16] these values were extracted from the Fermilab E835 data on fractional amplitudes of the electric dipole (E1), magnetic quadrupole (M2), and electric octupole (E3) transitions in the exclusive reactions $p\bar{p} \rightarrow \chi_{cJ} \rightarrow J/\psi \gamma \rightarrow e^+ e^- \gamma$, with $J = 1, 2$. They are listed here

$$r_0^1 = 0.498 \pm 0.032, \quad r_1^1 = 0.502 \pm 0.032, \tag{5.16}$$

$$r_0^2 = 0.075 \pm 0.029, \quad r_1^2 = 0.250 \pm 0.048, \quad r_2^2 = 0.674 \pm 0.052. \tag{5.17}$$

The corresponding values for a pure E1 transitions read $r_0^1 = r_1^1 = 0.5$, $r_0^2 = 0.1$, $r_1^2 = 0.3$, and $r_2^2 = 0.6$. Having these values we only need to calculate the independent components of $\rho_{\lambda\lambda'}^J$ to determine the J/ψ angular distribution $W^J(\theta, \phi)$ completely.

Analogously to Eq. (4.1), we can represent the angular distribution function as

$$W^J(\theta, \phi) = \frac{1}{2s} \int d^3 P S \cdot dW^J(\theta, \phi; \{\dots\}). \tag{5.18}$$

Such a representation will allow us to calculate correlations between kinematical variables of the central system as a whole (for example, rapidity y , momentum transfers $t_{1,2}$ and angle between outgoing protons ϕ_{pp}) and angular variables of produced J/ψ meson. Distributions $dW(\theta, \phi; \{\dots\})$ contain all the information about diffractive χ_c production mechanism, meson polarisations and decay process.

VI. GLUON OFF-SHELL EFFECTS

Let us comment now on the importance of gluon virtualities (transverse momenta) in the hard subprocess vertex $g^*g^* \rightarrow \chi_c(J^+)$ implied by the genuine k_t -factorisation scheme. This question was originally investigated in Ref. [9] when considering the central exclusive production of $\chi_c(0^+)$ meson. In particular, it was found that the on-shell approximation ($M_{\chi_c}^2 \gg q_{1,2}^2$) relying on the neglecting terms of the order of $q_{1,2}^2/M_{\chi_c}^2$ is too crude for the production of low mass systems with mass being of the order of a few GeV. In the $\chi_c(0^+)$ CEP case, inclusion of the gluon virtualities $q_{1,2}^2$ in the hard matrix element leads to a noticeable decrease of the total (bare) CEP cross section by a factor of 2 – 4 depending on the model of UGDF used.

This off-shell effect is even more pronounced in the case of the axial-vector $\chi_c(1^+)$ production, as it is dominated mostly by relatively large gluon virtualities and vanishes in the strict on-shell case. Even when included in the numerator of the vertex (see, e.g., Eq. (2.4)) the “small” terms $q_{1,2}^2$ are sometimes neglected in its denominator. Such an approximation $M_{\chi_c}^2 \gg q_{1,2}^2$ increases the total $\chi_c(1^+)$ CEP cross section by almost a factor of 7 in absolute normalization making a large effect in the $\chi_c(1^+)/\chi_c(2^+)$ ratio in the observable radiative decay channel [8] (see also Table I below). This resulted in a large discrepancy (in both normalisation of the total cross sections and relative spin contributions into observable signal) between our previous results in Refs. [7–9], where the exact hard matrix elements with off-shell gluons were used, and HKRS results in Refs. [4, 5], where gluon on-shell approximation $M_{\chi_c}^2 \gg q_{1,2}^2$ was adopted². Unlike the absolute normalisation of the cross section, the shapes of the differential distributions are not strongly affected by such an approximation.

One should note here that the description of the Tevatron data on the central exclusive χ_c production with updated results, including off-shell effects, becomes more difficult as the total cross section in the radiative decay channel $\chi_c(J^+) \rightarrow J/\psi + \gamma$ gets underestimated by about a factor of two with respect to the Tevatron data [8], if one uses values for the gap survival factors calculated in Refs. [4, 5]. However, such results are still within an overall theoretical uncertainty from the soft physics involved, UGDF models in the QCD mechanism under consideration [8], and also from unknown NLO corrections to the $g^*g^* \rightarrow \chi_c(1^+)$ vertex, which are implicitly, but only partly, taken into account by the k_t -factorisation approach used.

VII. SOFT RESCATTERING CORRECTIONS

In Refs. [7–9], for simplicity the whole analysis of observables has been performed adopting an approximation when all soft rescattering effects are effectively absorbed into the effective gap survival factor $\langle S_{\text{eff}}^2 \rangle$ taken into account multiplicatively. However, it is known from earlier analysis of the central exclusive Higgs production [6] (and later for unpolarized χ_c production [5]) that the soft rescattering may change angular distributions crucially, so it is not enough to include the gap survival factor as a constant normalization of the cross section.

In order to get some insight on the soft rescattering effects and include them dynamically,

² We are grateful to L. Harland-Lang for the significant help in understanding the major part of discrepancies between our calculations.

in the first approximation we use the simple one-channel model for the eikonal part of the survival probability calculated as

$$S_{\text{eik}}^2(\mathbf{p}_{1,t}, \mathbf{p}_{2,t}) = \frac{|\mathcal{M}^{\text{bare}}(\mathbf{p}_{1,t}, \mathbf{p}_{2,t}) + \mathcal{M}^{\text{res}}(\mathbf{p}_{1,t}, \mathbf{p}_{2,t})|^2}{|\mathcal{M}^{\text{bare}}(\mathbf{p}_{1,t}, \mathbf{p}_{2,t})|^2} \quad (7.1)$$

where $\mathbf{p}_{1/2,t}$ are the transverse momenta of the final protons, $\mathcal{M}^{\text{bare}}(\mathbf{p}_{1,t}, \mathbf{p}_{2,t})$ is the “bare” amplitude for the χ_c CEP, defined in Eq. (2.1), and $\mathcal{M}^{\text{res}}(\mathbf{p}_{1,t}, \mathbf{p}_{2,t})$ is the rescattering correction which can be written in the form (see, e.g., Eq. (13) in Ref. [17])

$$\mathcal{M}^{\text{res}}(\mathbf{p}_{1,t}, \mathbf{p}_{2,t}) \simeq \frac{iM_0(s)}{4\pi s(B+2b)} \exp\left(\frac{b^2|\mathbf{p}_{1,t} - \mathbf{p}_{2,t}|^2}{2(B+2b)}\right) \cdot \mathcal{M}^{\text{bare}}(\mathbf{p}_{1,t}, \mathbf{p}_{2,t}), \quad (7.2)$$

where $\text{Im}M_0(s) = s\sigma_{pp}^{\text{tot}}(s)$ (the real part is small in the high energy limit), B is the t -slope of the elastic pp differential cross section, and $b \simeq 4 \text{ GeV}^{-2}$ is the t -slope of the proton form factor. At the Tevatron energy we have $\sigma_{pp}^{\text{tot}} \simeq 80 \text{ mb}$ and $B \simeq 17 \text{ GeV}^{-2}$.

In Table I we have collected results for differential cross section $d\sigma_{\chi_c}/dy(y=0)$ for different spin states, as well as their contributions to the radiative $J/\psi + \gamma$ decay channel $d\sigma_{J/\psi\gamma}/dy(y=0)$ at Tevatron. For illustration, here we use only the perturbatively modeled KMR UGDF [6, 19], which include the Sudakov form factor and GRV94HO gluon PDF [20]. The results are presented for both versions of the absorptive corrections – by using the one-channel approximation according to the eikonal model³ (7.1), (7.2), and in the factorized form with \mathbf{p}_t -averaged (effective) gap survival factors $\langle S_{\text{eff}}^2 \rangle$ obtained recently in Ref. [5]:

$$\langle S_{\text{eff}}^2(\chi_c(0^+)) \rangle \simeq 0.0284, \quad \langle S_{\text{eff}}^2(\chi_c(1^+)) \rangle \simeq 0.0735, \quad \langle S_{\text{eff}}^2(\chi_c(2^+)) \rangle \simeq 0.0539, \quad (7.3)$$

where it is assumed that the enhanced suppression factor $\langle S_{\text{enh}}^2 \rangle = 0.49$ is the same for all spin states.

With the on-shell approximation $M_{\chi_c}^2 \gg q_{1,2}^2$ we basically reproduce the HKRS observable signal $\sim 0.7 \text{ nb}$ [5]. However, we see from Table I that keeping the exact matrix elements for the hard subprocess $g^*g^* \rightarrow \chi_c(J^+)$ (without the approximation $M_{\chi_c}^2 \gg q_{1,2}^2$ adopted in Refs. [4, 5]) it is rather difficult to get the Tevatron experimental value [2] $d\sigma^{\text{exp}}/dy|_{y=0}(pp \rightarrow pp(J/\psi + \gamma)) \simeq (0.97 \pm 0.26) \text{ nb}$, even by moving lower cut on the transverse momentum of the gluons in the loop $(q_{0,t}^{\text{cut}})^2$ down to the minimal perturbative scale 0.36 GeV^2 in GRV94HO gluon PDF [20]. This practically means that the central exclusive charmonia production is very sensitive to and seemingly dominated by yet unknown non-perturbative gluon dynamics at small x and q_t .

However, if we exclude the enhanced-diagram correction factor S_{enh} , which stands for QCD factorisation breaking in the considered QCD diffractive mechanism, we basically reproduce the Tevatron data and get the observable signal $\sim 0.94 \text{ nb}$ compared to the experimental value 0.97 nb . This may provide a clue that the QCD factorisation breaking effects may be overestimated and need further more careful attention.

One-channel eikonal model (7.2) is expected to provide the main effect on the shape of the distributions in the azimuthal angle Φ between outgoing protons shown in Fig. 2. Other distributions in meson rapidity y and momentum transfers along each proton line $t_{1,2}$ are

³ As for enhanced-diagram correction factor S_{enh} , we are grateful to L. Harland-Lang for providing us with a grid for its numerical calculation as a function of transverse momenta.

TABLE I: Differential cross section $d\sigma_{\chi_c}/dy(y=0)$ (in nb) of the exclusive diffractive production of $\chi_c(0^+, 1^+, 2^+)$ mesons and their partial and total signal in radiative $J/\psi + \gamma$ decay channel $d\sigma_{J/\psi\gamma}/dy(y=0)$ at Tevatron ($W = 1.96$ TeV) for the KMR UGDF [19], different cuts on the transverse momentum of the gluons in the loop $(q_{0,t}^{cut})^2$, with the on-shell gluons approximation $M_{\chi_c}^2 \gg q_{1,2}^2$ in the hard subprocess part (denoted as “on-shell”) and without it (“off-shell”). NLO correction factors to the hard part K_{NLO} [21] and absorptive corrections in factorized (7.3) and in one-channel model (7.1), (7.2) forms are included. Contributions of all polarisations are incorporated here.

UGDF approx.	$(q_{0,t}^{cut})^2$, GeV ²	$\chi_c(0^+)$		$\chi_c(1^+)$		$\chi_c(2^+)$		ratio		signal $\sum \frac{d\sigma_{J/\psi\gamma}}{dy}$
		$\frac{d\sigma_{\chi_c}}{dy}$	$\frac{d\sigma_{J/\psi\gamma}}{dy}$	$\frac{d\sigma_{\chi_c}}{dy}$	$\frac{d\sigma_{J/\psi\gamma}}{dy}$	$\frac{d\sigma_{\chi_c}}{dy}$	$\frac{d\sigma_{J/\psi\gamma}}{dy}$	$1^+/0^+$	$2^+/0^+$	
KMR, on-shell ^a $\langle S_{\text{eff}}^2 \rangle$	0.72	41.5	0.47	0.51	0.17	0.30	0.06	0.36	0.13	0.70
KMR, off-shell $\langle S_{\text{eff}}^2 \rangle$	0.72	10.3	0.12	0.06	0.02	0.14	0.03	0.17	0.25	0.17
KMR, off-shell $S_{\text{eik}}(7.2), S_{\text{enh}}$	0.36	29.4	0.34	0.13	0.05	0.36	0.07	0.15	0.21	0.46
KMR, off-shell $S_{\text{eik}}(7.2)$ only	0.36	60.0	0.69	0.27	0.10	0.73	0.14	0.15	0.21	0.94
HKRS [5]	0.72	35.0	0.40	0.71	0.24	0.45	0.09	0.61	0.22	0.73

^aIn order to avoid a confusion here, please, note this is not the rigorous on-shell case, but rather an approximation keeping the leading order term in $q_{1,2}^2/M_{\chi_c}^2$ -expansion.

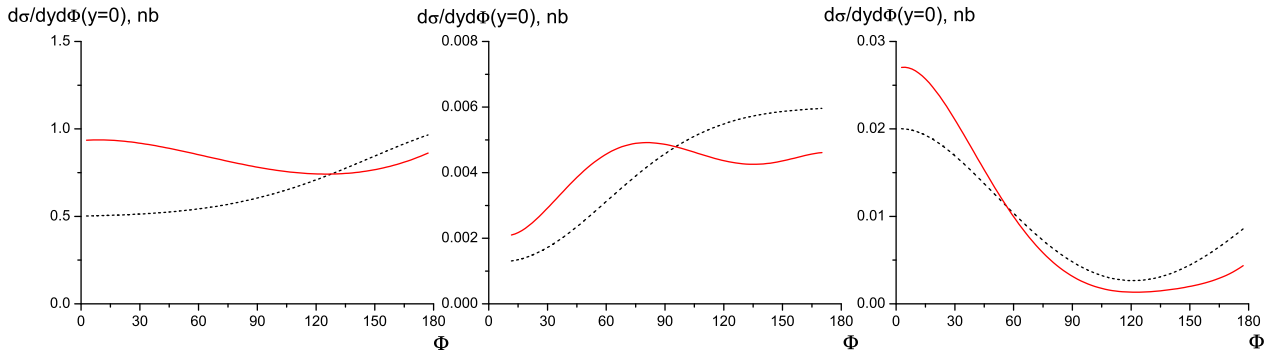


FIG. 2: Distributions in relative azimuthal angle Φ between outgoing protons of scalar $\chi_c(0^+)$ (left panel), axial-vector $\chi_c(1^+)$ (middle panel) and tensor $\chi_c(2^+)$ (right panel) mesons at $y=0$ taking into account absorptive corrections in the factorized form (7.3) (dotted lines) and in the one-channel model (7.1), (7.2) (solid lines) forms. KMR UGDF [19] was used.

not changed much – the effect in shapes is practically negligible. More general two-channel model [17] may lead to some corrections, but they are not so big, at least, in the realistic

phase space regions, we are interested in⁴.

VIII. CHARMONIUM POLARISATION EFFECTS IN THE HELICITY FRAME

Let us start from presenting differential cross sections. As was discussed in the previous Section, apart from the overall normalisation of the total cross section, the absorptive corrections can noticeably change the shape of distributions in the angle Φ between the final protons. As there is no way to measure the Φ -distributions yet, the measurable effect in Φ -integrated polarisation observables, which will be discussed below, can be effectively accounted for by the gap survival factors $\langle S_{\text{eff}}^2 \rangle$ listed in Eq. (7.3). For illustration purposes, we show results here only for “bare” distributions (without absorptive corrections) calculated with KMR UGDF [19]. In principle, absorptive corrections may differ for different elements of the helicity density matrix, and we leave the discussion of these effects for a future study.

In Fig. 3 we show distributions of the central exclusive $\chi_c(1^+)$ production cross section in the angle between outgoing protons Φ , momentum transfer t and meson rapidity y for different meson polarisations $\lambda = 0, \pm 1$. In Fig. 4 we present the same distributions for $\chi_c(2^+)$ meson production. Shapes in Φ and t are rather different for both mesons – at $y = 0$ $\chi_c(2^+)$ meson CEP is always dominated by helicity $\lambda = 0$, whereas $\chi_c(1^+)$ production is balanced by both $\lambda = 0$ and ± 1 contributions, and which is the dominating one depends on Φ and t phase space regions, we look at.

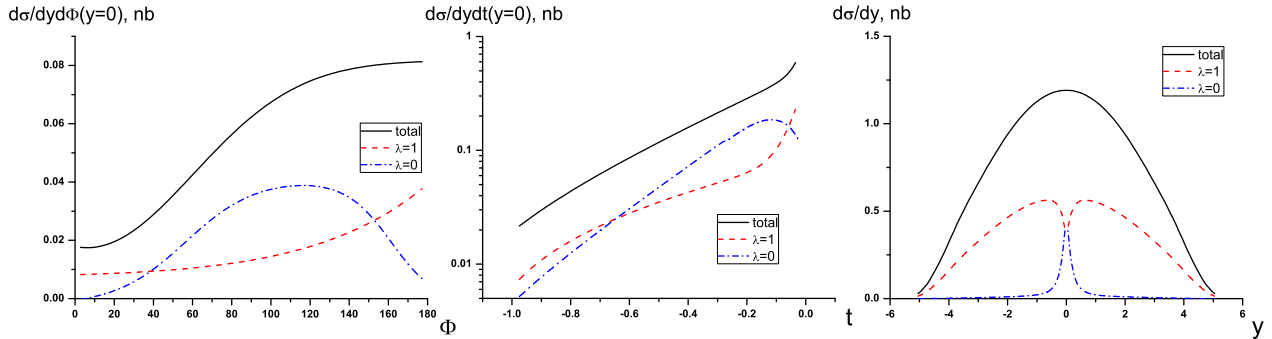


FIG. 3: Distributions of $\chi_c(1^+)$ CEP (bare) cross section in relative azimuthal angle Φ between outgoing protons (left panel), momentum transfer t along each proton line (middle panel) and meson rapidity y (right panel) for different meson helicities $|\lambda| = 0, 1$ (dash-dotted and dashed lines, respectively) and for the total (summed over all λ) CEP cross section (solid line). KMR UGDF [19] was used.

The cross sections integrated over all possible meson rapidities y (in our case $|y| \leq 6.0$) are dominated by maximal meson helicity contributions, i.e. by $|\lambda| = 1$ for $\chi_c(1^+)$ and by $|\lambda| = 2$ for $\chi_c(2^+)$ (see Tables II and III below). In the last case of tensor meson the $|\lambda| = 0$ and $|\lambda| = 1$ contributions turn out to have similar shapes in Φ and t and the same order of magnitude, however they are quite different at $y = 0$ as it is seen in Fig. 4.

Differential distributions for fixed meson polarisations in meson rapidity y , shown in Figs. 3 and 4 (right panels), exhibits maxima/minima in the central rapidity region $y \sim 0$

⁴ We are thankful to L. Harland-Lang for helpful discussions on this point.

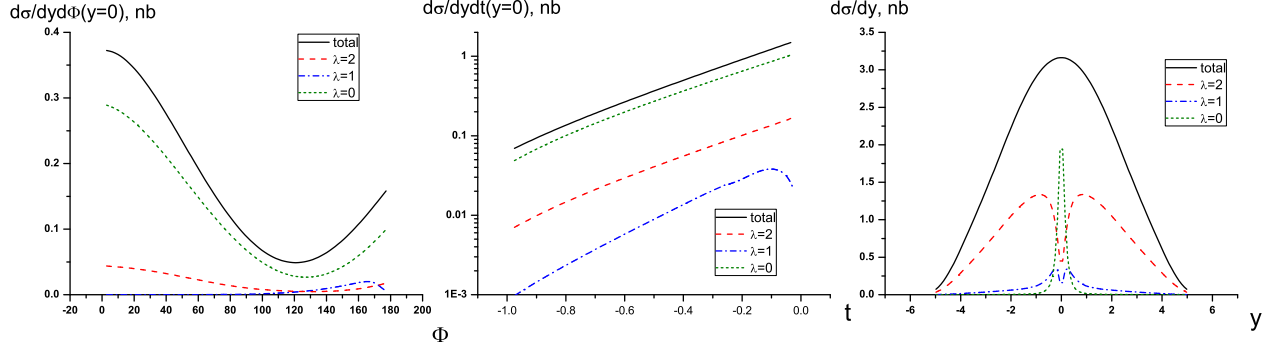


FIG. 4: Distributions of $\chi_c(2^+)$ CEP (bare) cross section in relative azimuthal angle Φ between outgoing protons (left panel), momentum transfer t along each proton line (middle panel) and meson rapidity y (right panel) for different meson helicities $|\lambda| = 0, 1, 2$ (short-dashed, dash-dotted and dashed lines, respectively) and for the total (summed over all λ) CEP cross section (solid line). KMR UGDF [19] was used.

similar to one presented in Fig. 1. Interestingly enough, these maxima/minima in partial helicity contributions cancel each other in the total (summed over all meson helicity states) cross section, which has a regular and smooth behavior around $y \rightarrow 0$. This is due to a non-trivial y -dependence of helicity amplitudes, which is a pure kinematical effect as discussed in Section III. Analogously, a non-trivial y -dependence of the hard $g^*g^* \rightarrow \chi_c(1^+, 2^+)$ subprocess amplitudes squared shown in Fig. 1 is canceled out in sums over all helicities λ resulting in Eq. (3.1). This confirms that the appearance of non-maximal helicities is a kinematical effect which is absent in the spin-averaged cross-section.

TABLE II: Non-zeroth integrated elements of the helicity matrix $\sigma_{\lambda\lambda'}^{J=1}$, $\lambda = 0, \pm 1$ (in nb) for exclusive $\chi_c(1^+)$ production at the Tevatron energy. KMR [19] and Kutak-Stásto UGDFs [18] have been used, absorptive corrections are not included. In the last column the ratio $\sigma_{00}^{J=1}/\sigma_{\chi_c}^{J=1} = \rho_{00}^{J=1}$ as a measure of subleading helicity-0 contribution to the total cross section is given.

UGDF	$\sigma_{00}^{J=1}$	$\sigma_{1,1}^{J=1}$	$\sigma_{1,0}^{J=1}$	$\sigma_{1,-1}^{J=1}$	$\rho_{00}^{J=1}$
KMR	0.27	3.54	$0.51 - 0.14i$	$-1.31 + 1.50i$	0.05
KS	0.49	3.92	$0.85 - 0.08i$	$-3.14 + 0.67i$	0.06

Apparently, such a kinematical effect in the CEP cross section depends on cuts in meson rapidity in a detector. It is a result of two competing asymptotical effects: heavy (non-relativistic, $y \rightarrow 0$) meson is dominantly produced in $\lambda = 0$ state, massless (relativistic, $y \gtrsim 1$) meson is produced mostly in $\lambda = \pm 1$ states. As a result of such a competition, it turns out that the central exclusive $\chi_c(1^+, 2^+)$ production cross sections are dominated by the second effect such that mostly relativistic charmonia (with large rapidities $y \gtrsim 1$) in a maximal helicity state are produced, so the detectors should be designed to be able to detect them (not only in the central rapidity region $y \sim 0$).

In Tables II and III we present the integrated elements of the diffractive $\chi_c(1^+, 2^+)$ production helicity matrix $\sigma_{\lambda\lambda'}^J = \sigma_{\chi_c}^J \rho_{\lambda\lambda'}^J$. Only independent, both diagonal (purely real) and

TABLE III: Non-zeroth integrated elements of the helicity matrix $\sigma_{\lambda\lambda'}^{J=2}$, $\lambda = 0, \pm 1, \pm 2$ (in nb) for exclusive $\chi_c(2^+)$ production at the Tevatron energy. KMR [19] and Kutak-Stasto UGDFs [18] have been used, absorptive corrections are not included. In the last column the ratio $\sigma_{00}^{J=2}/\sigma_{\chi_c}^{J=2} = \rho_{00}^{J=2}$ as a measure of subleading helicity-0 contribution to the total cross section is given.

UGDF	$\sigma_{00}^{J=2}$	$\sigma_{1,1}^{J=2}$	$\sigma_{2,2}^{J=2}$	$\sigma_{1,0}^{J=2}$	$\sigma_{2,0}^{J=2}$	$\sigma_{1,-1}^{J=2}$	$\sigma_{1,-2}^{J=2}$	$\sigma_{1,2}^{J=2}$	$\sigma_{2,-2}^{J=2}$	$\rho_{00}^{J=2}$
KMR	0.84	0.77	7.58	0.43	0.74	-0.54	1.37	1.93	5.0	0.05
KS	1.75	1.59	12.6	1.02	1.79	-1.38	3.17	3.95	8.3	0.06

non-diagonal (complex), non-zeroth elements are listed. Rapidity dependence of the non-diagonal terms (their real and imaginary parts) in the axial-vector $J = 1$ CEP case is presented for illustration in Fig. 5.

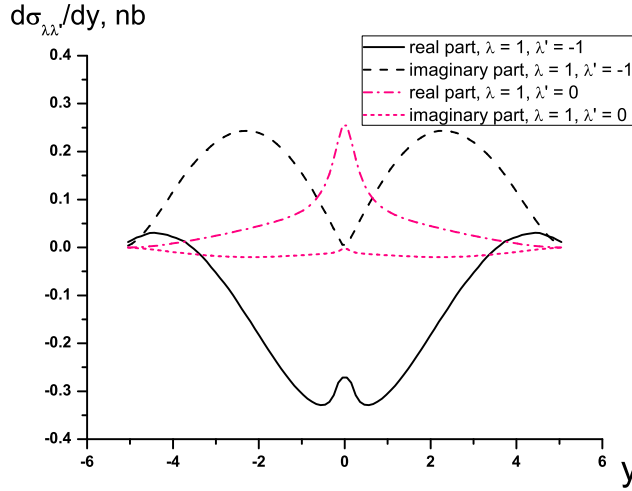


FIG. 5: Rapidity distributions of the independent non-diagonal elements of the helicity matrix $d\sigma_{\lambda\lambda'}^{J=1}/dy$ (real and imaginary parts) for the central exclusive axial-vector $\chi_c(1^+)$ meson production.

As was already pointed out, the total CEP cross section is dominated by the maximal helicities. The subleading contribution of states with $\lambda = 0$ in the total CEP cross section is about 5-6% for both $\chi_c(1^+)$ and $\chi_c(2^+)$ mesons. Measure of such subleading polarisation contribution is given by the ratio $\sigma_{00}^J/\sigma_{\chi_c}^J = \rho_{00}^J$ (see, last columns in Tables II and III). We calculated these ratios for two typical UGDF models: KMR [19] and Kutak-Stasto [18]. We see that the ratios $\rho_{00}^{J=1,2}$ are the same for both mesons, they are almost independent on UGDF models as the most of theoretical uncertainties (including soft rescattering effects) are canceled out inside them. Thus, ρ_{00}^J can be considered as a good model-independent observable for tests of underlined QCD production mechanism of χ_c mesons.

As it was demonstrated in Ref. [8], relative contributions of different spins J are rather sensitive to the model of UGDF. This is due to the fact that the central exclusive production of $\chi_c(1^+)$ is more sensitive to small gluon q_t than $\chi_c(2^+)$ production. Moreover, non-diagonal elements $\sigma_{\lambda\lambda'}^J$, $\lambda \neq \lambda'$ have much stronger sensitivity to UGDF model, than the diagonal ones. Therefore, experimental access to different elements of the production density matrix $\rho_{\lambda\lambda'}^J$ (or

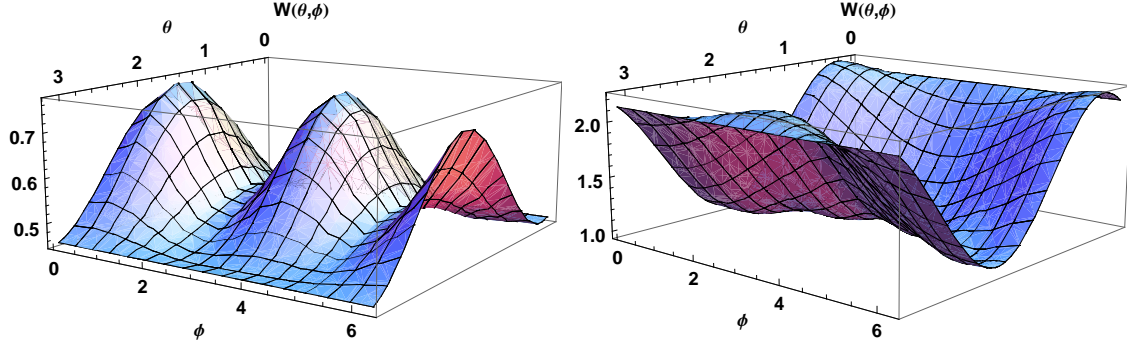


FIG. 6: Angular distribution $W(\theta, \phi)$ of J/ψ meson from radiative decay of centrally produced $\chi_c(1^+)$ (left panel) and $\chi_c(2^+)$ (right panel) mesons in polar θ and azimuthal ϕ angles in the helicity frame. Full phase space for central exclusive χ_c production is included, KMR UGDF [19] was used.

$\sigma_{\lambda\lambda'}^J$) would provide an opportunity for strong experimental constraints on the unintegrated gluon distributions at small x and small gluon transverse momenta q_t .

Now let us turn to the discussion of observable signal in radiative decay channel $\chi_c(1^+, 2^+) \rightarrow J/\psi + \gamma$. As one of the important characteristics of the production process $pp \rightarrow p(J/\psi\gamma)p$, the angular distribution of the J/ψ meson $W(\theta, \phi)$ in the helicity frame is shown in Fig. 6 as a function of polar θ and azimuthal ϕ angles for both $\chi_c(1^+, 2^+)$ mesons.

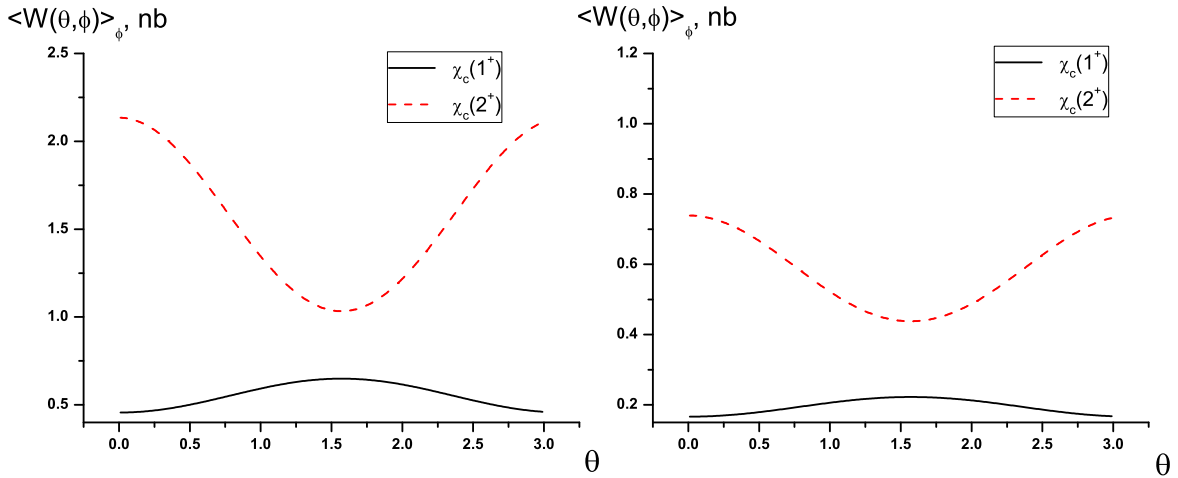


FIG. 7: Angular distribution of J/ψ meson averaged over azimuthal angle ϕ as function of polar angle θ (in radians) for $\chi_c(1^+)$ meson (solid line) and $\chi_c(2^+)$ meson (dashed line). Left panel corresponds to rapidity interval $|y| \leq 6$, right panel – to $|y| \leq 1$.

The function $W(\theta, \phi)$ is a periodic one in both the angles θ and ϕ . From Eqs. (5.13) and (5.14) it follows that the dependence on polar angle θ is determined mostly by the diagonal

terms of the production density matrix $\rho_{\lambda\lambda}^J$, whereas ϕ -dependence is given by real and imaginary parts of non-diagonal terms. Moreover, in the angular distribution $\langle W(\theta, \phi) \rangle_\phi$ averaged over ϕ all the terms with non-diagonal elements $\rho_{\lambda\lambda'}^J$, $\lambda \neq \lambda'$ are dropped out for both $\chi_c(1^+)$ and $\chi_c(2^+)$ mesons.

The ϕ -dependence of J/ψ meson from the $\chi_c(1^+)$ CEP turned out to be much stronger than that from $\chi_c(2^+)$ CEP as it is seen from Fig. 6. As for the θ -dependence, periods of oscillations for $\chi_c(1^+)$ and $\chi_c(2^+)$ mesons are shifted by $\pi/2$ with respect to each other, as demonstrated in Fig. 7 for distribution $\langle W(\theta, \phi) \rangle_\phi$ averaged over ϕ . Also, from this figure we see that the amplitudes of variations in θ become smaller and the dominance of the maximal helicity gets weaker and can be eliminated when one shrinks the rapidity interval in the phase space integral. This is a direct consequence of the specific rapidity dependence of the production density matrix elements in the central rapidity region $y \sim 0$.

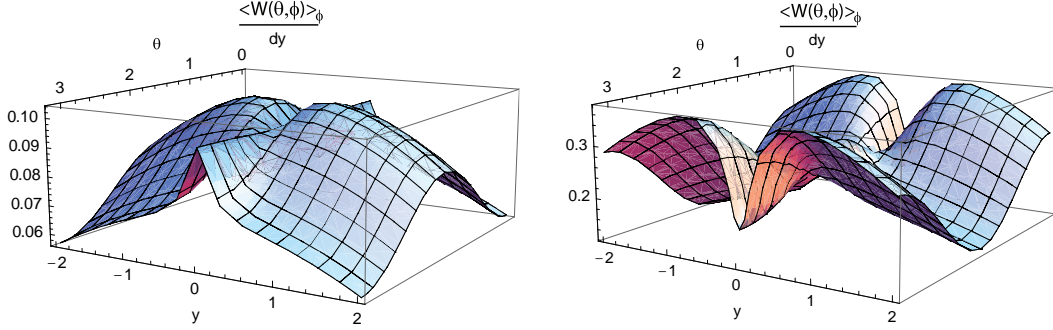


FIG. 8: Angular differential distribution of J/ψ meson averaged over azimuthal angle ϕ as function of polar angle θ (in radians) and χ_c meson rapidity y for $\chi_c(1^+)$ (left panel) and $\chi_c(2^+)$ mesons (right panel). KMR UGDF [19] was used.

Now the main question is how to measure experimentally the kinematical effects in the central exclusive $\chi_c(1^+, 2^+)$ production reflected in the maxima/minima of rapidity distributions $d\sigma_{\lambda\lambda}^J/dy$ for different meson helicities λ . Kinematical effects under consideration are natural in the helicity frame, in which we actually work⁵. Such a frame can be used in a real experiment. In principle, analogous calculations in other frames of reference can also be useful. As was already mentioned above, the total (summed over all meson helicities λ) cross section is regular around $y \sim 0$ and does not contain information about rapidity dependence of the partial helicity contributions.

Instead, for the purpose of experimental identification of the kinematical effects and separation of the meson helicity contributions it is instructive to look at the correlation function $d\langle W(\theta, \phi) \rangle_\phi/dy$ in both variables – polar angle of J/ψ meson and rapidity y of χ_c meson (or, equivalently, $J/\psi + \gamma$ system). We present such a function for each $J = 1, 2$ meson in Fig. 8. Maxima/minima in differential distributions $d\sigma_{\lambda\lambda}^J/dy$ are then reflected in y -dependence of the correlation function $d\langle W(\theta, \phi) \rangle_\phi/dy$ at fixed θ .

In principle, one can write formulae analogous to Eqs. (5.13) and (5.14) in another frame,

⁵ We are thankful to S. Baranov for useful discussion of this point.

where the “peaks” in rapidity near $y \sim 0$ can be eliminated. But then one loses some information about non-maximal helicity projections of the production density matrix. Since helicity has different meaning in different frames, our effect is purely of kinematical nature and thus should also be different in different frames.

IX. CONCLUSIONS AND DISCUSSION

Our results can be summarized as follows:

We have calculated differential cross sections for central exclusive $\chi_c(1^+, 2^+)$ meson production for different spin polarisations in the helicity frame. The integrated cross section for the maximal helicity state is approximately an order of magnitude greater than that for the non-maximal ones. We have shown that this effect has a kinematical nature: heavy (non-relativistic, $y \rightarrow 0$) meson is dominantly produced in the $\lambda = 0$ state, massless (relativistic, $y \gtrsim 1$) meson is produced mostly in the $\lambda = \pm 1$ states. In the total cross section integrated over the meson rapidity y the second effect turns out to be dominated, i.e. relativistic with $y \gtrsim 1$ χ_c mesons with maximal helicity ($\lambda = \pm 1$ for $\chi_c(1^+)$ and $\lambda = \pm 2$ for $\chi_c(2^+)$) are preferably produced in the exclusive process $pp \rightarrow p\chi_c p$.

We used two different models for the q_t -dependent unintegrated gluon distributions from the literature – conventional KMR distribution which includes Sudakov form factor [19] and the nonlinear Kutak-Staśto model [18] based on unified BFKL-DGLAP evolution. The contributions of the minimal helicity state $\lambda = 0$ given by the diagonal elements of the production density matrix $\rho_{00}^{J=1,2}$ are close both $\chi_c(1^+, 2^+)$ mesons and amount to 5 – 6 %. They are only weakly dependent on UGDF (but rather strongly dependent on cuts in rapidity y). Such quantities $\rho_{00}^{J=1,2}$ are, therefore, good model-independent observables, which can be used to constrain the underlying QCD diffractive production mechanism of heavy quarkonia.

We have calculated, in addition, angular distributions of J/ψ meson $W(\theta, \phi)$ from radiative decays $\chi_c(1^+, 2^+) \rightarrow J/\psi + \gamma$ in the helicity frame, both analytically and numerically. The function $W^J(\theta, \phi)$ contains an important information about all independent elements of the production density matrix $\rho_{\lambda\lambda'}^J$, both diagonal and non-diagonal. Azimuthal angle ϕ dependence of outgoing J/ψ mesons is given by the real and imaginary parts of the non-diagonal elements $\rho_{\lambda\lambda'}^J$, $\lambda \neq \lambda'$, which are very sensitive to the UGDF model used. A specific shape of the rapidity dependence of the J/ψ meson correlation function $d\langle W^J(\theta, \phi) \rangle_\phi / dy$ shown in Fig. 8 is a result of the “peaked” shape of the χ_c production density matrix around central rapidity region $y \sim 0$. Measurements of such a differential distribution $d\langle W^J(\theta, \phi) \rangle_\phi / dy$ averaged over azimuthal angle ϕ would allow to separate different helicity contributions and to identify the kinematical effects under discussion. Distributions based on general correlation function $W^J(\theta, \phi)$ can, in principle, be measured at the Tevatron and LHC. They could also provide an independent check of the discussed diffractive QCD mechanism.

Acknowledgments

This work was partly supported by the Carl Trygger Foundation, the RFBR (grants No. 09-02-01149 and 09-02-00732) and the Polish grant of MNiSW No. N202 2492235. We are grateful to Sergey Baranov and Valery Khoze for valuable and stimulating discussions. We

are especially indebted to Lucian Harland-Lang for the exchange of Fortran codes, making possible a direct comparison of our calculations and to find out the reasons of differences between them.

-
- [1] M. G. Albrow *et al.* [FP420 R and D Collaboration], JINST **4**, T10001 (2009) [arXiv:0806.0302 [hep-ex]].
 - [2] T. Aaltonen *et al.* [CDF Collaboration], Phys. Rev. Lett. **102**, 242001 (2009) [arXiv:0902.1271].
 - [3] M. G. Albrow, T. D. Coughlin and J. R. Forshaw, arXiv:1006.1289 [hep-ph].
 - [4] L. A. Harland-Lang, V. A. Khoze, M. G. Ryskin and W. J. Stirling, Eur. Phys. J. C **65**, 433 (2010) [arXiv:0909.4748 [hep-ph]].
 - [5] L. A. Harland-Lang, V. A. Khoze, M. G. Ryskin and W. J. Stirling, arXiv:1005.0695 [hep-ph].
 - [6] V.A. Khoze, A.D. Martin and M.G. Ryskin, Phys. Lett. B **401**, 330 (1997);
V.A. Khoze, A.D. Martin and M.G. Ryskin, Eur. Phys. J. C **23**, 311 (2002);
A.B. Kaidalov, V.A. Khoze, A.D. Martin and M.G. Ryskin, Eur. Phys. J. C **31**, 387 (2003) [arXiv:hep-ph/0307064];
A.B. Kaidalov, V.A. Khoze, A.D. Martin and M.G. Ryskin, Eur. Phys. J. C **33**, 261 (2004);
V.A. Khoze, A.D. Martin, M.G. Ryskin and W.J. Stirling, Eur. Phys. J. C **35**, 211 (2004).
 - [7] R. S. Pasechnik, A. Szczurek and O. V. Teryaev, Phys. Lett. B **680**, 62 (2009) [arXiv:0901.4187 [hep-ph]].
 - [8] R. S. Pasechnik, A. Szczurek and O. V. Teryaev, Phys. Rev. D **81**, 034024 (2010) [arXiv:0912.4251 [hep-ph]].
 - [9] R. S. Pasechnik, A. Szczurek and O. V. Teryaev, Phys. Rev. D **78**, 014007 (2008) [arXiv:0709.0857 [hep-ph]].
 - [10] C. S. Lam and W. K. Tung, Phys. Rev. D **18**, 2447 (1978).
 - [11] V. A. Khoze, A. D. Martin and M. G. Ryskin, Eur. Phys. J. C **19**, 477 (2001) [Erratum-ibid. C **20**, 599 (2001)] [arXiv:hep-ph/0011393].
 - [12] B. A. Kniehl, D. V. Vasin and V. A. Saleev, Phys. Rev. D **73**, 074022 (2006) [arXiv:hep-ph/0602179].
 - [13] B. A. Kniehl, G. Kramer and C. P. Palisoc, Phys. Rev. D **68**, 114002 (2003) [arXiv:hep-ph/0307386].
 - [14] H. Pilkuhn, *The Interactions of Hadrons*, (North-Holland, Amsterdam, 1967), p. 222.
 - [15] J. J. Sakurai, *Modern Quantum Mechanics*, (Addison-Wesley, Reading, 1994), p. 223.
 - [16] E835 Collaboration, M. Ambrogiani *et al.*, Phys. Rev. D **65**, 052002 (2002).
 - [17] V. A. Khoze, A. D. Martin and M. G. Ryskin, Eur. Phys. J. C **24**, 581 (2002) [arXiv:hep-ph/0203122].
 - [18] K. Kutak and A.M. Staśto, Eur. Phys. J. C **41**, 341 (2005).
 - [19] M. A. Kimber, A. D. Martin and M. G. Ryskin, Phys. Rev. D **63**, 114027 (2001) [arXiv:hep-ph/0101348];
A. D. Martin and M. G. Ryskin, Phys. Rev. D **64**, 094017 (2001) [arXiv:hep-ph/0107149].
 - [20] M. Glück, E. Reya and A. Vogt, Z. Phys. C **67**, 433 (1995);
M. Glück, E. Reya and A. Vogt, Eur. Phys. J. C **5**, 461 (1998).
 - [21] R. Barbieri, M. Caffo, R. Gatto and E. Remiddi, Nucl. Phys. B **192**, 61 (1981);
W. Kwong, P. B. Mackenzie, R. Rosenfeld and J. L. Rosner, Phys. Rev. D **37**, 3210 (1988);

M. L. Mangano and A. Petrelli, Phys. Lett. B **352**, 445 (1995) [arXiv:hep-ph/9503465].